Interaction dynamics in small networks of nonlinear elements

Michael Stich[*,a], Manuel G. Velarde[a]

[a]*Instituto Pluridisciplinar; Universidad Complutense de Madrid; Paseo Juan XXIII, 1; 28040 Madrid; Spain.*

Abstract

We study a small circuit of coupled nonlinear elements to investigate general features of signal transmission through networks. The small circuit itself is perceived as building block for larger networks. Individual dynamics and coupling are motivated by neuronal systems: We consider two types of dynamical modes for an individual element, regular spiking and chattering and each individual element can receive excitatory and/or inhibitory inputs and is subjected to different feedback types (excitatory and inhibitory; forward and recurrent). Both, deterministic and stochastic simulations are carried out to study the input-output relationships of these networks. Major results for regular spiking elements include frequency locking, spike rate amplification for strong synaptic coupling, and inhibition-induced spike rate control which can be interpreted as a output frequency rectification. For chattering elements, spike rate amplification for low frequencies and silencing for large frequencies is characteristic.

Key words: Signal transmission, small networks, integrate-and-fire neurons

1. Introduction

In many areas of science and engineering, we are facing the problem of information transmission and amplification, independently whether we are studying metabolic cell networks, neuronal communication, or artificial information systems like the internet. The topological structure of such systems in many cases is characterized by networks of individual elements. However, the size and complexity of such systems lead to a hierarchical organzation of such systems, in the sense that what appears as an individual element on a given level, is actually formed by a subsystem with its own dynamics on a lower level.

In this article, we study a small circuit of coupled nonlinear elements to investigate general features of signal transmission through networks. The small circuit itself is perceived as building block for larger networks. As motivation and for the sake of specificity, we choose the individual dynamics and the coupling similar as in neuronal systems. The nervous system is the most efficient biologically-evolved information transmission system. To understand how it encodes, transmits and decodes information is of prime relevance,

*Corresponding author. Present address: Non-linearity and Complexity Research Group, SEAS, Aston University, Aston Triangle, Birmingham B4 7ET, UK.
Email address: m.stich@aston.ac.uk (Michael Stich)

not only for neuroscientists, but also for those who want to use a neuro-inspired architecture to engineer information processes. Therefore, it is important to study how the dynamic properties of the signals, typically in the form of action potentials, are transformed as they propagate through a neural network. A single neuron may receive excitatory and inhibitory inputs of thousands of different neurons, and finally emits a signal that after being processed locally, represents (at least partially) the information contained in the input. In the processes that change the dynamic properties of the signals, crucial roles are played by the difference between excitatory and inhibitory signals, the ubiquitous presence of noise, and frequency and phase properties of the spike trains [1, 2]. This so-called coding problem for the understanding of real and specific neural systems is conceptually opposite to the approach to engineer, implement, and control the time-dependent signal transmission properties of a artificial network of neurons. Here, we construct small networks of neurons where each neuron has well-known autonomous dynamics, and we study how the signals (action potentials) that it receives are converted into an output signal and how the latter depends on the network topology. Nevertheless, since these artificial networks can be also designed to model real data, both approaches are finally closely related.

In this article, we want to understand, how the spike rates of one or two neurons depend (a) on their autonomous state (either regular spiking or chattering), (b) on the input (excitatory or excitatory plus inhibitory), (c) on the character of the synaptic coupling between the two neurons (feedforward or recurrent). To model the single-neuron dynamics, a simple model adaptable for both regular spiking and chattering neurons is used [3]. To account for small random variations of the input currents, noise is incorporated into the model equations. We focus on two neurons because it is well known that already small networks of neurons are able to generate complex behavior due to their coupling within the network [4]. Such a small network may serve as a building block for larger systems and could be implemented in electronic circuits.

2. Model

Let us consider a system formed by two neurons. For each neuron with index i, it reads

$$\dot{v}_i = 0.04v_i^2 + 5v_i + 140 - u_i + I_i + \sqrt{2D_i}\,\xi(t)\,, \tag{1a}$$

$$\dot{u}_i = a(bv_i - u_i)\,. \tag{1b}$$

The model is based on the one proposed by Izhikevich [3]. The variables v and u mimick the membrane potential and membrane recovery, respectively. The synaptic (or externally injected) current to a neuron is represented by I. The parameter a characterizes the time scale of the membrane recovery and the parameter b how strong the recovery is build up. The model is scaled such that the membrane potential v corresponds

to values in mV and the time to values in ms. The firing event is described by a cutoff condition given by

$$\text{if } v_i = 30 \text{ then } \begin{cases} v_i = c\,, \\ u_i = u_i + d\,, \end{cases} \tag{2}$$

where c and d are parameters describing the reset of the membrane potential and the recovery variable, respectively. To the dynamics of the neurons we add an equation for the synaptic currents, given by equation

$$I_j = \sum_{\text{all } i} |s_{ji}|\, g_i(E_i - v_j), \tag{3}$$

where j denotes the postsynaptic neuron and i the presynaptic one. The matrix of synaptic connectivity is given by s_{ji}. The function g represents the synaptic conductance, behaving according to

$$\dot{g}_i = -0.2 g_i\,. \tag{4}$$

This equation mimicks the approximately exponential decay of the conductance with a characteristic time scale of 5 ms (resembling typical values for excitatory AMPA and inhibitory GABA$_\text{A}$ concentrations [5]). Each time the presynaptic neuron i fires, its conductance g_i increases, which is described by

$$\text{if } v_i = 30 \text{ then } g_i = g_i + 1\,. \tag{5}$$

The function E represents the reversal potential of the presynaptic neuron:

$$E_i = \begin{cases} 0 & \text{for an excitatory neuron,} \\ -90 & \text{for an inhibitory neuron.} \end{cases} \tag{6}$$

Note that in Eq. (3) the sum is taken over all connected neurons and that g usually is nonzero. Therefore, a neuron j continuously receives a synaptic current I_j with different contributions from all presynaptic neurons i. Note that the current between the pre- and postsynaptic neuron depends (a) on the state of the presynaptic neuron – if it is excitatory or inhibitory (E_i) and if it is firing (g_i large) or not, (b) the general coupling strength between the neurons (s_{ji}), and (c) the momentary state of the postsynaptic neuron: since usually $v_j > -90$, a presynaptic inhibitory neuron creates negative postsynaptic currents while a presynaptic excitatory neuron creates positive postsynaptic currents, at least while $v_j < 0$. Although the postsynaptic currents are in general small, their magnitude becomes large if a presynaptic neuron fires.

Within the model, the reversal potential E completely determines whether a neuron has an excitatory or inhibitory impact. Nevertheless, for convenience we assign positive (negative) numbers to excitatory (inhibitory) connections in the matrix s_{ji}.

In order to take into account small current fluctuations we include an additive noise term for the potential v (which is the independent variable). The parameter D_i characterizes the magnitude of the Gaussian white

noise affecting all neurons described by $\langle \xi(t)\xi(t') \rangle = \delta(t-t')$. The value D_i is only given if different from zero (stochastic simulations). Fluctuations of the electric current are present in all real systems (both neuronal and artificially implemented) and are necessarily additive in this model. We are not primarily interested in noise-induced effects (such as stochastic resonance), and also not discuss situations under which other noise terms (such as multiplicative noise) arise.

3. Numerical methods

The numerical integration of the model (1-6) is done with Euler and fourth-order Runge-Kutta schemes. While the Euler method is chosen for stochastic simulations, the Runge-Kutta scheme is used for deterministic simulations. To decrease the numerical error introduced by the cutoff condition, we use an interpolation method for integrate-and-fire neurons where the firing times are determined to higher precision [6]. We have found that integration time steps may be chosen up to one order of magnitude larger with this algorithm. Typical integration time steps are $\Delta t = 0.025$ ms for Runge-Kutta, and $\Delta t = 0.0025$ ms for Euler.

The network consists of one or two neurons subjected to one or two external inputs. We assume that the network of study is embedded in a larger neural network, suggesting that the input to the neurons consists of spike trains. For simplicity, these spike trains are created with the same equations that describe the dynamics of the neurons, with the difference that the current I_0 is constant in time and therefore is used as a control parameter. There are two independent inputs: an excitatory input (the corresponding "neuron" is labeled with index 0) and an inhibitory one (labeled with index 3). Since I_0 is constant in time, the resulting spike train is periodic. For $I_0 < 4$, the input neuron remains silent. As I_0 is increased above this value, periodic spiking sets in. Then, the spike rate increases approximately linearly with the input current as $r \approx 2.15\,I_0$ s^{-1} (see below Fig. 2(a)). Thus, for the given set of parameter values, the system describes a Type-II excitability dynamics. In the simulations, the input current is changed from $I_0 = 4.5$ up to $I_0 = 55.0$ in steps of 0.5. We either display the results as functions of the input spike rates r_0 (deterministic simulations) or the input currents I_0 (stochastic simulations).

The neurons, labelled with indices 1 and 2, are in their excitable regime, i.e. without input they are in their rest state. Below, we report results obtained from simulations for networks of regular spiking (RS) and chattering (CH) neurons. The parameters of a RS neuron are $a = 0.02$, $b = 0.2$, $c = -65$, $d = 8$ and those of a CH neuron $a = 0.02$, $b = 0.2$, $c = -50$, $d = 2$ [3]. We express our results in terms of the spike-count rate r_i (sometimes also called frequency) and with help of histograms of interspike intervals (ISI) for binsizes 0.5 ms. For most simulations, the simulated time interval is chosen to be 40 s (20 s for CH neurons).

We investigate a total of six different network topologies, described in Fig. 1, differing in the number of inputs (1 or 2), number of neurons (1 or 2), and the type of coupling between them. The basic one is depicted in (a), where an excitatory input enters neuron 1. This type of input is present in all schemes and

hence represents a central driving force to the network. In (b), neuron 1 is an excitatory neuron for neuron 2. In scheme (c), there is an additional inhibitory spike train affecting both neuron 1 and 2. In (d) that inhibitory spike train only enters neuron 2. In (e) we have an inhibitory feedback from neuron 2 to neuron 1, and finally in (f), an excitatory feedback to neuron 1.

4. Results

4.1. Regular spiking neurons: single-neuron case

First, we investigate the input-output relationship for one neuron, i.e. the spike-count rate of neuron 1 as a function of the input frequency, for an excitatory connection between the input and the neuron. Since we start with the deterministic system, a perfectly periodic spike train with controlled frequency is created. Figure 2(b) shows the input-output relationship for neuron 1 for a synaptic coupling $s_{10} = 0.3$. For low input frequencies, the output spike rate is identical to the input frequency, i.e. every input spike leads to an output spike. However, as the input frequency goes beyond a critical value, here approximately 24 s^{-1}, the output spike rate decreases. As the input frequency is increased further, the output spike rate increases and decreases alternately. The reason for this behavior is that a neuron has an intrinsic inertial dynamics and therefore it is unable to follow the fast input.

Although the output spike rate is a nonmonotonic function of the input frequency, the ratio of the two spike rates shows monotonic behavior. In Fig. 2(c) we see that for a wide range of values of the input frequency, the ratio between the input and output frequencies is an integer number k. The corresponding spike trains show one outgoing spike for k incoming spikes. This phenomenon is denoted as $k : 1$ frequency locking. In Fig. 2(b), the locking behavior is reflected by a linearly increasing output spike rate where the slope is $1/k$. Also, there are input frequencies where the output spike train does not show the perfect simple-periodic behavior of the input spike train but displays higher periodicities associated with other ratios (3:2, 5:2, etc.). Generally, there is $m : n$ locking (m, n integer numbers) found in the system, although for simplicity we restrict our analysis here to the case of $k : 1$ locking with k integer. Quasiperiodic and chaotic regimes may be expected but have not been explored in the present study.

In the presence of noise, the spike rate is best characterized by ISI histograms. Figure 2(d) shows the gray scale coded ISI histograms for neuron 1 for different values of the input current I_0. Since the number of spikes observed in a fixed time interval depends on I_0, we rescale the gray scale for each value of I_0, i.e., for each simulation. We observe that for the noise level and parameters chosen, the interspike intervals are uni- or bimodal. To compare the result with Fig. 2(c), we divide the interspike intervals by the mean value of the ISI of the input. In this way, we obtain Fig. 2(e), a normalized ISI histogram. It can be seen that where the original ISI distribution is unimodal, $k : 1$ frequency locking is observed. In the presence of noise, locking refers to the mean values and we shall refer to this as stochastic frequency locking. Constructing the

normalized ISI histogram, any n-modal structure of the original histogram is conserved. Therefore, there are also wide ranges of the input spike rate where the corresponding ISI histogram is bimodal. These ranges correspond to the regions *between* different $k : 1$ locking regions.

Let us now discuss the effect of the strength of the synaptic coupling on the spike rate of the neuron in the absence of noise. We have seen that neuron 1 can be locked to the input spike train. How does locking behavior depend on the coupling strength? We can anticipate that the stronger the coupling, the more faithful will neuron 1 follow the input. This is shown in Fig. 3(a) for three coupling strengths. For $s_{10} = 0.2$, the spike rate at which the locking breaks down is close to $15.7 \, \text{s}^{-1}$, for $s_{10} = 0.3$, it is 24.5, and for $s_{10} = 0.4$, it is 33. Simulations for other intermediate coupling strengths (data not shown) confirms this tendency which means that the critical rate changes approximately linearly with the coupling strength. Besides this effect, we observe that curves behave qualitatively similar, i.e., once the 1:1 coupling is lost, the spike rate decreases until it is locked to the input spike rate in other ratios. To analyze this situation a little further, we rescale the rate r_1 for each coupling value by its rate at $r_0 = 130 \, \text{s}^{-1}$ (strictly speaking at $I_0 = 60$) which is a very large value for the applicability range of a RS neuron. By dividing through that value, we obtain the curves displayed in Fig. 3(b). From these curves we extract the information that independently of the coupling strength, the spike rate at which the 1:1 locking breaks down has an approximately constant ratio to its value at $r_0 = 130 \, \text{s}^{-1}$, around 84%. Rephrasing that finding, this means that neuron 1 reaches 84% of its accessible frequency range through a low frequency input to which it locks 1:1.

To understand the aspect of the coupling strength, in Fig. 3(c), we display the spike rate ratios of the curves of Fig. 3(a). We see that for stronger coupling, neuron 1 can follow the input more faithfully, while for weaker coupling, neuron 1 is detached earlier from the input. While we have seen this already in Fig. 3(a), we observe furthermore that neuron 1 still can lock efficiently up to a locking of 7:1 which demonstrates that its dynamics may be very slow but still clearly dependent to the input. These results can be understood if we recall that for low values of s_{10} the synaptic currents are smaller and the neuron has a reduced tendency to fire. Therefore, it is more inertial and decouples more easily from the input dynamics. On the other hand, for a strong coupling the neuron is able to follow the input spike trains up to higher input frequencies.

By varying the coupling strength systematically, we are able to obtain an overview of the locking regions. Figure 3(d) shows the result. Area 1 denotes the 1:1 locking region. As the upper boundary of this region is crossed, the spike rate drops down until $r_1 = 0.5 r_0$, which represents the transition to 2:1 locking (entering region 2). Only the curve denoting the upper boundary of region 1 shows approximately linear behavior for increasing s_{10} (i.e., the rate at which 1:1 locking breaks downs scales linearly with the coupling strength) while the other curves seem to show only linear behavior for small s_{10} and rise stronger for large s_{10}. The curves do not intersect here and this means that the slope of a curve limiting a locking region increases with k. Therefore, the frequency range of the locking regions for a given k indeed increases with s_{10}, as noted above. This figure also illustrates that a given input spike train with frequency r_0 can lead to a range of

output spike trains, depending on the synaptic coupling strength. Note that for $s_{10} < 0.12$ no input spike train with $r_0 < 100$ s^{-1} leads to an output spike train. It is reasonable to interpret this as an effective critical coupling strength for information transmission for the neurons (for the given parameter set). This parameter is hence critical for a possible implementation in electronic circuits.

4.2. RS neurons: two-neuron system with feedforward topology

The results presented above have been obtained for a single neuron subjected to an excitatory input. Let us now add a second neuron, which is coupled in an excitatory way to neuron 1, i.e. with $s_{21} > 0$. First, no inhibitory input is present and the only input to neuron 2 is the spike train emitted by neuron 1.

In Fig. 4(a) we display the results of two series of simulations that clarify how serial forward coupling with different synaptic strengths influences the input-output relationship. We have a fixed connection strength $s_{10} = 0.3$ and explore what effects take place as we modify the connectivity s_{21}.

If the coupling s_{21} is large, the spike rate r_2 is equal to the spike rate r_1 for practically the whole range of input frequencies r_0. Therefore, 1:1 frequency locking between neuron 1 and 2 is observed. However, for high input spike rates, neuron 2 has a lower frequency than neuron 1. If, on the other hand, s_{21} is small, neuron 2 decouples from neuron 1 already at $r_1 \approx 15$ s^{-1} and remains at lower spike rates for the rest of the input frequency range. These effect are visualized better in Fig. 4(b) where we plot r_1/r_2 as a function of r_0. For large s_{21}, r_1/r_2 is identical to 1, and then it deviates continuously from 1 to slightly larger values, however, without showing a clear locking behavior. We come back to that curve further below. For smaller s_{21}, the curve is actually non-monotonic, but shows clearly regimes with 3:2 and 2:1 locking.

What happens to a feedforward network if the coupling strength is the same for both neurons, but varies in absolute magnitude? The answer is displayed in Fig. 4(c) for $s_{21} = s_{10} = 0.5$ and 0.7. For comparison, we include the curves for $s_{21} = s_{10} = 0.3$ from Fig. 4(a). The main observation, 1:1 coupling for a wide range of r_0 is repeated. Furthermore, we see that the frequency at which the locking breaks down is not a simple function of the connectivity. The most striking new finding here is that for large synaptic strengths, neuron 1 can actually have a higher spike rate than the input and accordingly (since coupling strengths are equal), neuron 2 can actually produce more spikes than neuron 1. This represents a frequency amplification which is due to the fact that the input current of a neuron in nonzero also if the presynaptic is not firing. This implies that the line that limits the 1:1 locking region in Fig. 3(d) is not exactly correct for large couplings.

To understand the soft and monotonic increase of r_1/r_2 for strong coupling Fig. 4(b), we have performed stochastic simulations and in Fig. 4(d) we display the corresponding normalized ISI histograms. It can be seen that stochastic frequency locking 1:1 is observed for almost the whole range of considered I_0 (note that also the histograms of neuron 1 are bimodal and therefore neuron 2 may show stochastic frequency locking 1:1 with neuron 1 also in the bimodal regime). Only for $I_0 > 45$, deviations from 1:1 locking are found. Then, neuron 2 falls behind the pace given by neuron 1: There is a cloud of points appearing around

2, representing twice as large ISIs as for neuron 1. Accordingly, the relative decrease in spike-count rate displayed in Fig. 4(a) means that occasionally a spike of neuron 1 cannot give rise to a firing of neuron 2. This tendency becomes more and more dominant as the input spike rate is increased.

4.3. RS neurons: two-neuron system with inhibition

Until now, we have discussed a network of one or two neurons with one input spike train for neuron 1. Let us now consider the case of an additional inhibitory input spike train. We fix the frequency of the incoming excitatory spike train and study the dynamics of neuron 1 and neuron 2 as the spike rate of the incoming inhibitory spike train is increased. Inhibition influences neuron 1 directly and neuron 2 directly and through neuron 1. The results of deterministic simulations are shown in Fig. 5(a,b) for two different initial conditions.

In absence of inhibition, the output spike rate of neuron 2 (solid lines) would be equal to the one of neuron 1 (dashed lines) and equal to the input frequency, $r_0 = 22.4$ s^{-1} (dotted lines). Let us first discuss the dynamics of neuron 1. As the frequency of the inhibitory spike train is increased, the spike rate of neuron 1 decreases until for $r_3 \approx 44$ s^{-1} no spike train is generated anymore. However, there is a region around the frequency of the excitatory input, i.e. $r_3 \approx r_0$ s^{-1}, where the spike rate of neuron 1 may be equal to the frequency of the excitatory input (Fig. 5(a)) or zero (Fig. 5(b)). The difference lies in the relative phase of the incoming spike trains (the simulation is deterministic): if an excitatory spike arrives first, it may create a spike and the inhibitory spike does not produce an effect on the spike dynamics of the neuron. However, if an inhibitory spike arrives just before the excitatory spike, the latter cannot produce a spike and the neuron remains silent. This phase relationship can be quantified by t_0, which describes the time delay of the inhibitory spike with respect to the excitatory spike in the initial condition. It is $t_0 = 9.4$ (a) and $t_0 = 43.0$ (b). Of course, the relative phase of the incoming spike trains does only lead to a global effect if the frequencies of the excitatory and inhibitory spike trains are close to each other. If their frequencies are different, the effects wash out for the long integration time intervals considered here. Neuron 2 receives the output spike train of neuron 1 and additionally the inhibitory spike train directly. The results demonstrate that additional inhibition reduces the output spike rate. For low r_3, the effect is weak, leading to a frequency decrease of 5-10%. For inhibitory input spike rates larger than $r_3 \approx 22.4$s^{-1}, the effect is increasingly larger ($\approx 20\%$) until finally the neuron 2 stops firing for lower spike rates than in the case without the additional inhibition.

Finally, we consider a network formed by two neurons where neuron 2 is subjected to an inhibitory spike train of fixed frequency $r_3 = 43$ s^{-1} (ISI= 23 ms) and to an excitatory spike train of variable frequency originated in neuron 0 and transmitted through neuron 1. Noise is present in the simulations shown in Fig. 5(c,d). The ISI histograms of neuron 0 and neuron 1 are qualitatively similar to the one presented in Fig. 2(d). However, the ISI histograms of neuron 2, displayed in Fig. 5(c), show a multimodal structure

which changes strongly as I_0 is changed. The most prominent mode is typically that with relatively small ISI while subharmonic modes have a smaller magnitude. A closer inspection reveals that the ISI histogram of neuron 2 is only unimodal if the histogram of neuron 1 is unimodal. Neuron 2 takes its lowest ISI already for low input frequencies (e.g., $I_0 = 8$), whereas in the absence of noise the lowest ISI is reached only asymptotically for very high input frequencies. Indeed, the most frequently observed interspike intervals cluster around ISI= 46 ms, which represents the half of the frequency of the inhibitory spike train. Thus, as I_0 is changed, the spike rate of neuron 2 only changes very little. For example, between $I_0 = 27$ and $I_0 = 34$, the histograms of neuron 2 are practically unimodal and the frequency is almost constant. Therefore, as the frequency of the excitatory input spike train is modified, the output frequency remains constant. On the other hand, if the input current is changed from $I_0 = 27$ to $I_0 = 26$, the output frequency is changed drastically. If we divide the ISI histograms by the mean input ISI (and create the normalized ISI histograms), as shown in Fig. 5(d), we see instead of plateaus almost straight lines with constant slope. Therefore, no frequency locking with the excitatory input frequency is observed. Neuron 2 seems to prefer a 2:1 locking with the inhibitory frequency.

4.4. RS neurons: 2-neuron system with recurrent feedback

In this part, we investigate two types of network topology which have attracted strong interest due to their presence in real neural networks, e.g., in the context of Central Pattern Generators [7]. One type represents recurrent inhibition, i.e. a neuron inhibits the source of its own excitation and the other recurrent excitation, i.e. a neuron excites the source of its own excitation. Here, we discuss the simplest case of a recurrent network, where neuron 1 excites neuron 2 and neuron 2 provides a feedback to neuron 1.

In Fig. 6, we compare three simulations. First, we include a simulation that has already been shown above: the excitation of neuron 2 by neuron 1 through a connection with weight $s_{21} = 0.3$ and no recurrent feedback present ($s_{12} = 0$, dotted lines). Second, the spike train emitted by neuron 2 serves as additional excitatory input to neuron 1 ($s_{12} = 0.3$, dashed lines). Third, the recurrent feedback is inhibitory ($s_{12} = -10$, solid lines).

Without feedback, neuron 1 and neuron 2 are locked 1:1 for input spike rates up to approximately 97 s^{-1}. We can see from both, spike rates and their ratios that recurrent inhibition extends the frequency region where 1:1 locking takes place, while recurrent excitation narrows the respective region. For input frequencies larger than approximately 60 s^{-1}, recurrent excitation leads to an increased firing rate of neuron 1 and a decreased spike rate of neuron 2. Figure 6(b) reveals that this is associated with a 2:1 locking between neuron 1 and neuron 2. Note that in this case, the spike rate of neuron 2 is lower than for the cases with inhibition or absence of recurrent input. It should be mentioned that in the excitatory case and very small input frequencies (below 10 s^{-1}), the spike rates of both, neuron 1 and neuron 2 may be larger than the input spike rate. An interesting feature of the dynamics of the network with recurrent inhibition is that the

spike rate is approximately constant for frequencies between 97 s^{-1} and 110 s^{-1}. In summary, recurrent inhibition seems to stabilize the 1:1 locking and therefore synchronization of the small neural network while excitation leads to a fast and a slow spiking neuron which are locked 2:1.

4.5. Chattering neurons

In this section, we present results for simulations performed for chattering (CH) neurons. There, spikes appear in bursts (typically of 3-5 spikes) [8] and which is relatively short compared to other bursting neurons of bursting type. Between the spikes, the membrane potential stays on a high level. In Fig. 7(a) we show the spike frequency as a function of the constant current I_0 for an isolated neuron. Again, the spike frequency is defined as the number of spikes divided by the considered time interval (here $\Delta t = 20$s). As for the RS neuron, the spike frequency increases in quite a linear fashion with the current. Of course, the spike frequency is much higher since several spikes form a single chattering event (burst). Two basic regimes must be distinguished. For small currents, the neuron is indeed chattering and a burst consists of an increasing number of spikes while for large currents (larger than $I_0 \approx 22$), the neuron converts into a continuously spiking neuron. In the regime for low currents, the frequency curve reflects the number of spike per chattering event. The first point describes a burst with 3 spikes; the next 5 points represent bursts with 4 spikes; the next 5 points reflect bursts with 5 spikes; the next 4 points describe bursts with 6 spikes and finally the next 3 points represent bursts with 7 spikes. The increase in spike rate going from a burst of, e. g., 3 spikes to one with 4 spikes is partially compensated by the decrease of the frequency of the burst. Therefore, the overall increase in spike rate is relatively small.

Now, the dynamics of an autonomous neuron can be studied as its excitatory input consists of a chattering neuron. Figure 7(b) shows the results of corresponding simulations. The spike rate of neuron 1 is shown as a function of the input spike rate for different values of the coupling constant. The main results are the following: (i) In general, the spike rate increases with input frequency. However, there is a abrupt decrease in frequency as the input switches from the chattering regime to the continuously spiking regime (thus independent of the coupling constant, just dependent on the qualitative shape of the input spike train). Note that for the considered coupling strengths, the spike train of neuron 1 (if produced at all) always stays in the regime of chattering. (ii) The stronger the excitatory coupling from the input to neuron 1, the larger is the output spike rate. (iii) The thin line describes 1:1 locking. For $s_{10} = 0.10$ and $s_{10} = 0.15$, there is an interval where 1:1 locking is observed. (iv) For small input frequencies and strong coupling (dotted line), the output spike rate may be larger than the input spike rate (thin solid line for comparison).

To illustrate this result, we show in Fig. 7(c,d) the temporal development of two networks of two CH neurons with different synaptic coupling strengths subjected to the same chattering input. In Fig. 7(c) a typical situation is seen where the spike train of neuron 1 (solid line) shows less spikes per burst than the input spike train (dotted line). The coupling between the input and neuron 1 and neurons 1 and 2 is

relatively weak and therefore the output of neuron 2 does not show any spikes (dashed line). Note that there is a significant delay of approx. 12 ms between the first spike of the input and the first spike of neuron 1. Also, there is a delay of approx. 7 ms between the last incoming spike and the first spike of neuron 1. Figure 7(d) displays a simulation where the input again consists of 3 spikes, whereas neuron 1 generates 4 spikes and neuron 2 even 5 spikes. Hence, such strong coupling can lead to the amplification of signals. The delay between the first spikes of input and neuron 1 is much smaller, here approx. 4 ms.

Going back to Fig. 7(b), we see that for relatively small input frequencies of approx. 50 - 150 s^{-1} the frequency of neuron 1 behaves nonmonotonic in a similar way as observed for the RS neurons (Fig. 2(b)). This holds for all considered coupling strengths, although the effect is more pronounced for strong coupling.

As mentioned above, the output spike rate abruptly decreases as the input spike train switches from chattering to a continuously spiking behavior. One could see this as a natural limit for a CH, because to describe a fast spiking neuron, other parameter choices for a, b, c or d are appropriate. Nevertheless, we consider this case here: For weak coupling ($s_{10} = 0.05$), neuron 1 may even cease to fire as the fast spiking behavior sets in (solid curve in Fig. 7(b)). Furthermore, as the input frequency is increased further, the spike rate of neuron 1 sharply jumps from zero to approx. 16 s^{-1}.

Actually, in the simulations presented in Fig. 7(b), the spike train of neuron 1 was further injected into neuron 2. In the following, we study the dynamics of this network in detail. In Fig. 8 we show how the temporal behavior of neuron 2 depending on the input frequency for different coupling strengths. In Fig. 8(a), neuron 1 is weakly coupled to the input ($s_{10} = 0.05$) and the spike rate is shown as thick solid line. For weak coupling between neuron 1 and 2 (dotted line), neuron 2 shows a very weak response, with occasionally no spikes and never producing an output exceeding 15 s^{-1}. Without characterizing this dynamics further, it seems as if this is not a reliable regime for information transmission which implies that it should be avoided in an electronic implementation. For intermediate coupling (dashed line), neuron 2 follows the pace of neuron 1 for the wide ranges of the input frequency. For strong coupling (dot-dashed line), the frequency of neuron 2 lies above the frequency of neuron 1. Of course, if neuron 1 is silent, neuron 2 cannot produce a spike train either. Beyond the regime where $r_1 = 0$, the increase of $r_{1,2}$ is rather regular, but this is already in a regime where the input is continuously firing instead of chattering and therefore not of mayor interest here.

In Fig. 8(b), neuron 1 is moderately coupled to the input ($s_{10} = 0.10$) and r_1 is again shown for comparison as thick solid line. Also here, neuron 2 ceases to fire occasionally for weak couplings to neuron 1 and seems below a critical coupling strength for reliable signal transmission. However, even for strong couplings the spike rate of neuron 2 usually does not exceed the one of neuron 1. Exceptions are very small input frequencies and the frequency range just after the abrupt decrease. This has also been observed for regular spiking neurons (results not shown). However, since this may represent a situation where other networks and parameters (e.g., networks with neurons of different types) may be appropriate, the details of

11

this behavior have not been investigated. In contrast to Fig. 8(a) we see that the spike rate rather decreases (or stays constant) than increases as the input spike train is in the regime of fast spiking.

Finally, Fig. 8(c) presents the case where neuron 1 is strongly coupled to the input. Also here, the spike rate of neuron 2 drops down to zero for weak couplings (however, in the frequency range where the input is already in the purely spiking regime). Now, the spike rate of neuron 2 is only larger than the one of neuron 2 for small input frequencies. Again, the spike rate slightly decreases for high input rates and even reaches levels below the regime of chattering input. Since we only changed the coupling from the input to neuron 1, and kept coupling strengths between neuron 1 and 2 constant throughout Fig. 8, we see that once neuron 1 produces a spike rate of $r_1 \approx 40$ or larger in the regime where the input is continuously spiking, neuron 2 shows only a very weak dependence on the spike rate of neuron 1. This may indicate that a CH neuron as a receptor of a fast spiking neuron cannot discriminate well between different spike rates.

The next step in the study of this system consists of investigating the dependence of the spike rate of neuron 2 as a function of the coupling s_{10} for different coupling strengths s_{21}. In Fig. 9(a) we show for weak coupling between neuron 1 and neuron 2 ($s_{21} = 0.05$), how the spike rate depends on the input spike rate for three different coupling strengths s_{21}. The three curves are rather flat and low and show only small variability (especially in the low-frequency range) although the respective spike rates of neuron 1 differ significantly. As already suggested by the findings displayed in Fig. 9(a), a coupling strength of $s_{ij} = 0.05$ seems to small to be efficient for coupled CH neurons. Figure 9(b) displays the corresponding curves for intermediate coupling between neuron 1 and neuron 2 ($s_{21} = 0.10$). Also here, the curves are rather flat, but the variability for small input rates is only a little smaller than the variability of the curves for neuron 1. Finally, Fig. 9(c) illustrates the findings for strong coupling ($s_{21} = 0.15$). There, neuron 2 follows the pace of neuron 1 stronger and the output may have a larger spike rate than neuron 1. Nevertheless, the overall results of these simulations is that the spike rate of neuron 2 depends rather strongly on the coupling to neuron 1 and rather weakly on the spike rate of neuron 1.

5. Discussion

We have investigated a small network of two coupled neurons. The dynamics of single neurons is described by a model proposed by Izhikevich [3]. In spite of its simplicity and in contrast to other reduced models, it seems to be able to reproduce all dynamical regimes known for Hodgkin-Huxley neurons [9]. We studied two types of neurons, Regular Spiking (RS) and Chattering (CH) neurons.

First, the network consisted of two RS neurons which receive an incoming excitatory spike train. The input spike rate has been varied between 7 s^{-1} and 130 s^{-1}. This range falls within the frequency range measured for human RS neurons (up to 150 s^{-1} in transients and 50 s^{-1} in steady state asymptotics [7]).

We have investigated the input-output relationship in absence and presence of noise. We have shown

that the spike rate can decrease even for increasing input spike rate. We have found frequency locking phenomena between input and output spike trains and determined the boundaries of the main locking regions $k : 1$ in a phase diagram for input frequency and synaptic coupling. We have seen that the locking regions depend approximately linearly on the synaptic coupling strength and that a postsynaptic RS neuron can reach approximately 84% of its asymptotic frequency (at 130 s^{-1}) in a 1:1 frequency locking with its input independent of the coupling strength. We have shown that as long as $s_{10} > 0.12$, the postsynaptic neuron behaves in a coherent signal processing way even for weak coupling (and hence low output frequency). The frequency and locking behavior agrees qualitatively well with experimental data (e.g., Ref. [10]).

The stochastic simulations revealed more details about the locking behavior. In the $k : 1$ locking regions, the ISI diagram is unimodal. Between these regions (and including other lockings like 3:2), the ISI distribution is bimodal, at least in first approximation and for low input frequecies. However, as the input frequency becomes larger, the distribution becomes broader and broader.

The impact of an additional inhibitory input has been explored. Generally, inhibition lowers the output spike rate or even makes the neuron silent. However, the relative phase of the inhibitory spike train to the excitatory spike train plays a crucial role if the spike rates of the excitation and inhibition are similar (resonance effect).

Furthermore, we have observed that for some ranges of the input frequency and in the presence of noise, the output spike rate may remain practically constant. Within these ranges, the neuron is insensitive to changes of the input spike rate. Inhibition may therefore give rise to a constant output signal for small variations of the spike rate of the incoming spike train while at the same time allowing for the possibility of generating different modes of output, if the spike rate is changed significantly. This an interesting observation since this implies that the inhibitory spike train can play the role of a rectifier.

Mainly for the purpose of comparison, we have performed deterministic simulations of the same network topologies (although not all of them) for chattering neurons. Since a chattering neuron shows a temporal dynamics on two time scales (a short interspike interval within a burst, a long time interval between bursts), the temporal behavior is very different than a regular spiking neuron. However, for low input frequencies, the qualitative coding dynamics is similar in that we observe frequency locking. A novel feature is that as the input spike train switches from a chattering mode to a fast spiking mode, the postsynaptic neuron, in spite of being coupled in an excitatory way, decreases strongly its activity, and may even cease to fire. This feature can be called silencing. For faster input spike trains the neuron re-ignites, but its spike rate remains almost constant once the direct input exceeds $r \approx 40$ s^{-1}. Both effects together demonstrate that chattering neurons do not efficiently process intermediate or high-frequency inputs. As for regular spiking neurons, as the coupling is very strong, the postsynaptic frequency may be larger than the presynaptic one. However, since this may represent a situation where other networks and parameters (e.g., networks with neurons of different types) may be appropriate from a biological point of view. However, these limitations do not apply

if an artificial network is formed by nonlinear elements governed by such input-output dynamics. Then, this effect may be used to amplify signals and therefore could be possibly useful in an electronic implementation.

Acknowledgments

References

[1] F. Rieke, D. Warland, R. de Ruyter van Steveninck, Spikes: Exploring the Neural Code, MIT Press, Cambridge, 1999.

[2] P. Dayan, L. F. Abbott, Theoretical Neuroscience, MIT Press, Cambridge, 2001.

[3] E. M. Izhikevich, Simple model of spiking neurons, IEEE Trans. Neural Net. 14 (2003) 1569–1572.

[4] J. Milton, Dynamics of Small Neural Populations, American Mathematical Society, Providence, 1996.

[5] A. Destexhe, Z. Mainen, T. Sejnowski, Synthesis of models for excitable membranes, synaptic transmission and neuro-modulation using a common kinetic formalism, J. Comput. Neurosc. 1 (1994) 195–230.

[6] D. Hansel, G. Mato, C. Meunier, L. Neltner, On numerical simulations of integrate-and-fire neural networks, Neural Comp. 10 (1998) 467.

[7] H. R. Wilson, Spikes, decisions, and actions, Oxford University Press, Oxford, 1999.

[8] C. M. Gray, D. A. McCormick, Chattering cells: Superficial pyramidal neurons contributing to the generation of synchronous oscillations in the visual cortex, Science 274 (1996) 109–113.

[9] E. M. Izhikevich, Which model to use for cortical spiking neurons?, IEEE Trans. Neural Net. 15 (2004) 1063–1070.

[10] H. Hayashi, S. Ishizuka, Chaotic responses of the hippocampal CA3 region to a mossy fiber stimulation in vitro, Brain Res. 686 (1995) 194–206.

Figure captions

Figure 1. The network topologies studied. An excitatory input to neuron 1 is always present. (a) 1 excitatory input, 1 neuron. (b) 1 excitatory input, 2 neurons (excitatory feedforward). (c) 1 excitatory, 1 inhibitory input, 2 neurons (excitatory feedforward). (d) as (c), but the inhibitory input influences only neuron 2. (e) as (b) but with an inhibitory feedback. (f) as (b) but with excitatory feedback.

Figure 2. (a) The spike rate of the input r_0 as created by a constant current I_0. (b-e) Input-output relationship for neuron 1. The synaptic coupling is $s_{10} = 0.3$ and the noise level is zero (a,b) and $D_i = 0.5$ (c,d). (b) Dependence of the spike-count rate r_1 on the input frequency r_0. (c) Ratio of the spike-count rates as a function of the input frequency. (d) ISI histograms for different I_0. Dark areas represent high spike rates. (e) Normalized ISI histograms (see text).

Figure 3. (a,b) Input-output relationship for neuron 1 for different coupling strengths, $s_{10} = 0.2$ (dashed line), $s_{10} = 0.3$ (solid line), and $s_{10} = 0.4$ (dot-dashed line). In (a) we show r_1 as function of r_0. In (b) we show the same date where each curve is rescaled with its value at $r_0 = 130$ s^{-1}, called r_{1max}. (c,d) Frequency locking. (c) Ratio of the input and output spike rate as a function of the input frequency for different synaptic coupling strengths $s_{10} = 0.2$ (dashed line), $s_{10} = 0.3$ (solid line), and $s_{10} = 0.4$ (dot-dashed line). (d) Locking regions for a RS neuron. The regions 1-4 denote $k : 1$ locking with $k = 1, 2, 3, 4$, respectively.

Figure 4. Excitatory feedforward. (a) Spike rates for neurons 1 and 2. The synaptic coupling is $s_{10} = 0.3$ (neuron 1 is solid curve) and we show neuron 2 for two different coupling strengths ($s_{21} = 0.3$, dotted curve) and $s_{21} = 0.2$, dashed curve). (b) Same data for the spike ratio r_1/r_2 showing the locking regions. (c) Spike rates for neurons 1 and 2 for three cases: $s_{21} = s_{10} = 0.3$ (see also (a), solid thin and thick curves), $s_{21} = s_{10} = 0.5$ (dotted thin and thick curves), $s_{21} = s_{10} = 0.7$ (dashed thin and thick curves). (d) Normalized ISI histograms for $s_{21} = s_{10} = 0.3$. $D_0 = 0.5$.

Figure 5. Influence of inhibitory (a,b) and inhibitory-plus-excitatory (c,d) input. (a,b) Neuron 1 (dashed lines) and neuron 2 (solid lines). The parameters are $s_{10} = s_{21} = 0.3$, $s_{13} = s_{23} = -10$. t_0 describes the time delay of the inhibitory spike with respect to the excitatory spike in the initial condition: $t_0 = 9.4$ (a) and $t_0 = 43.0$ (b). The period of the excitatory spike train is $T = 44.6$ ($I_0 = 10.5$). (c) ISI histograms for different I_0. (d) Normalized ISI histograms. The parameter values are $I_3 = 20$ (corresponding to $\langle \text{ISI} \rangle = 23$ ms and $\langle r_3 \rangle = 43$ s^{-1}), $D_0 = D_1 = D_2 = 0.5$ and $s_{10} = 0.3$, $s_{21} = 0.6$, $s_{23} = -10$.

Figure 6. Recurrent excitation and inhibition. (a) Spike rates of neuron 1 and neuron 2 for $s_{10} = 0.3$ and different values of s_{12}. (b) Ratios of the input and output spike rate as a function of the input frequency.

Figure 7. (a) Dependence of the spike frequency on a constant input current for a CH neuron. The parameters of a CH neuron are $a = 0.02$, $b = 0.2$, $c = -50$, $d = 2$. (b) Spike rate of a CH neuron 1 as a function of input frequency (also CH neuron) for different coupling strengths (s_{10}). The thin solid line shows the input frequency for comparison. (c,d) Temporal behavior of CH neurons. Input: dotted line, neuron 1: solid line, neuron 2: dashed line. (c) $I_0 = 4$, $s_{10} = s_{21} = 0.05$. (d) $I_0 = 4$, $s_{10} = s_{21} = 0.15$.

Figure 8. Spike rates of neuron 2 as a function of the input frequency for a network of CH neurons. The thick solid lines correspond to the neuron 1 lines in Fig. 7(b). (a) $s_{10} = 0.05$, (b) $s_{10} = 0.10$, (c) $s_{10} = 0.15$.

Figure 9. Spike rates of neuron 2 as a function of the input frequency for a network of CH neurons for different couplings s_{21}. The thin lines correspond to the neuron 1 lines in Fig. 7(b). (a) $s_{21} = 0.05$, (b) $s_{21} = 0.10$, (c) $s_{21} = 0.15$.
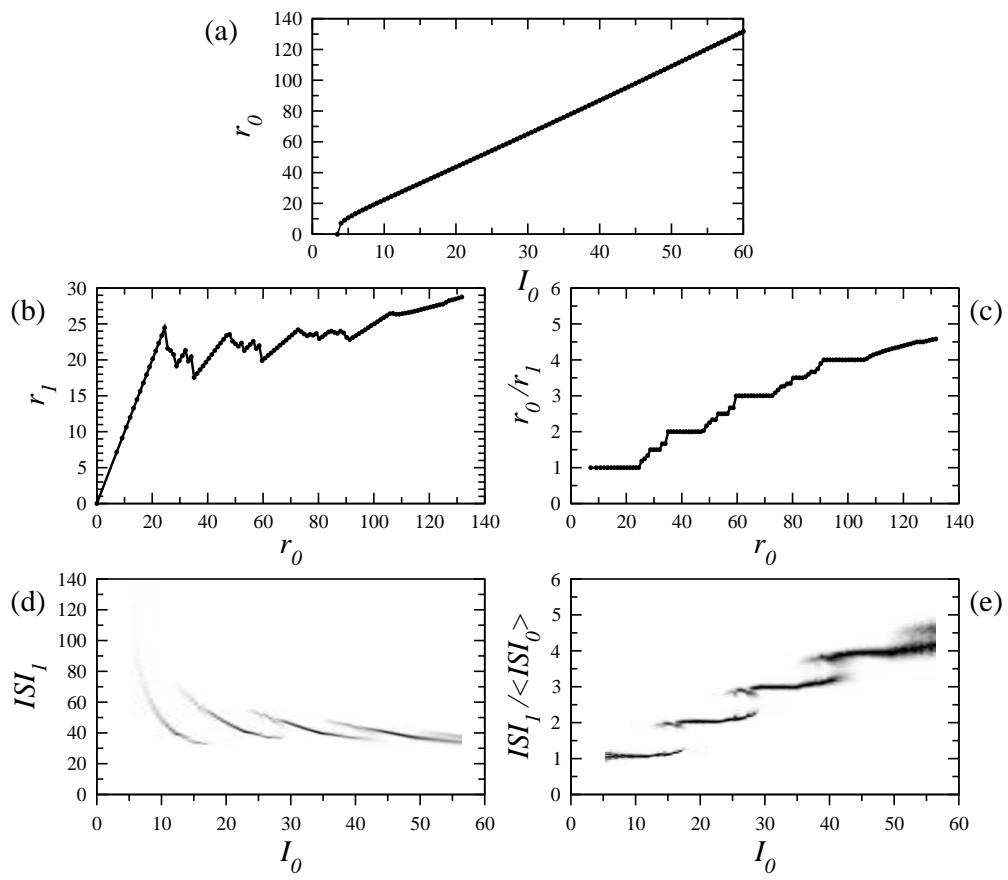
(a)
excitatory input
s_{10}
1
neuron 1

(b)
excitatory input
s_{10}
1
s_{21}
2
neuron 1
neuron 2

(c)
input 1 (exc.)
input 2 (inh.)
s_{10}
s_{13}
s_{23}
1
s_{21}
2
neuron 1
neuron 2

(d)
input 1 (exc.)
input 2 (inh.)
s_{10}
s_{23}
1
s_{21}
2
neuron 1
neuron 2

(e)
excitatory input
s_{10}
s_{12}
1
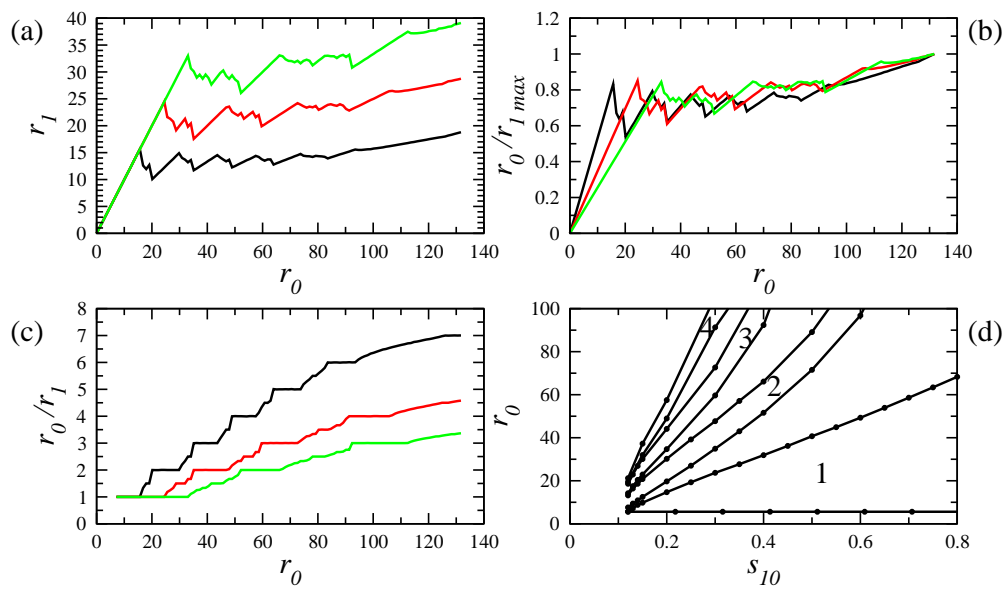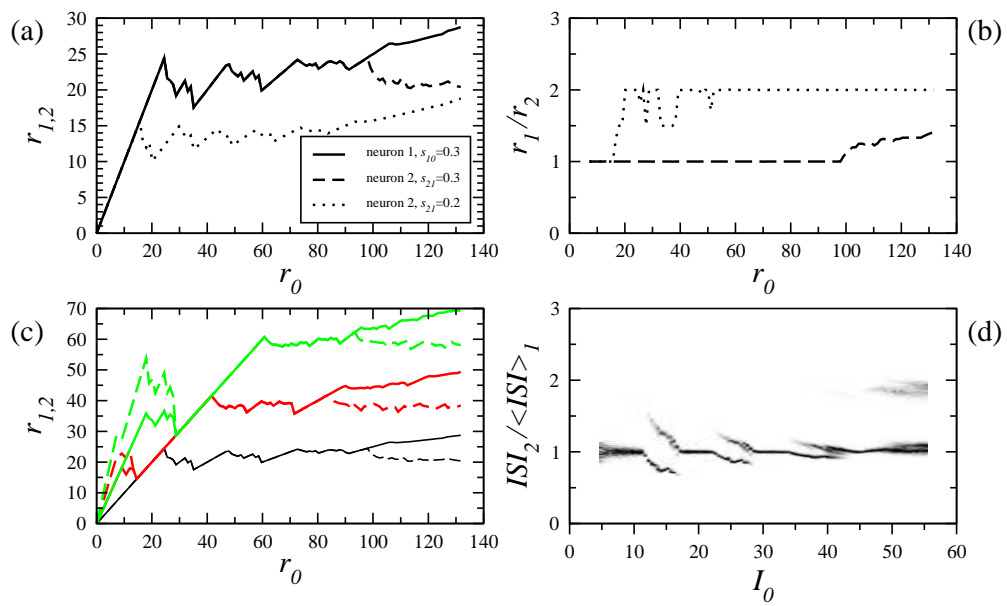s_{21}
2
neuron 1
neuron 2

(f)
excitatory input
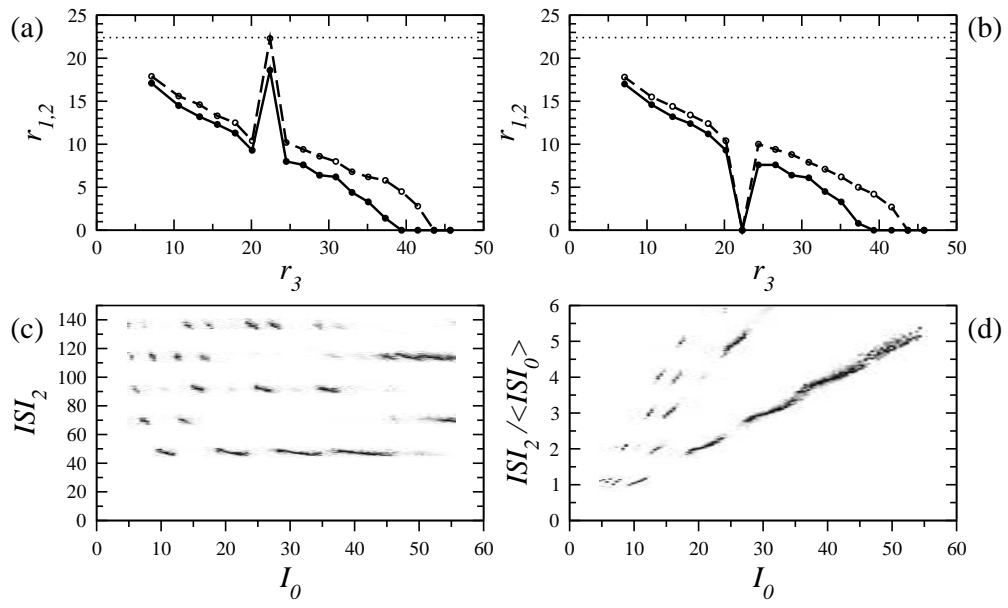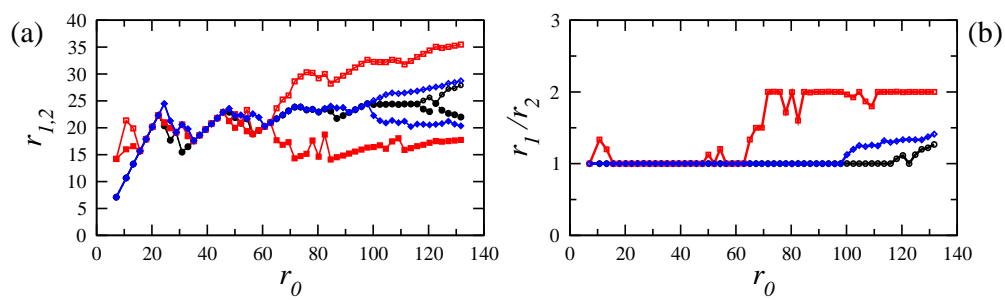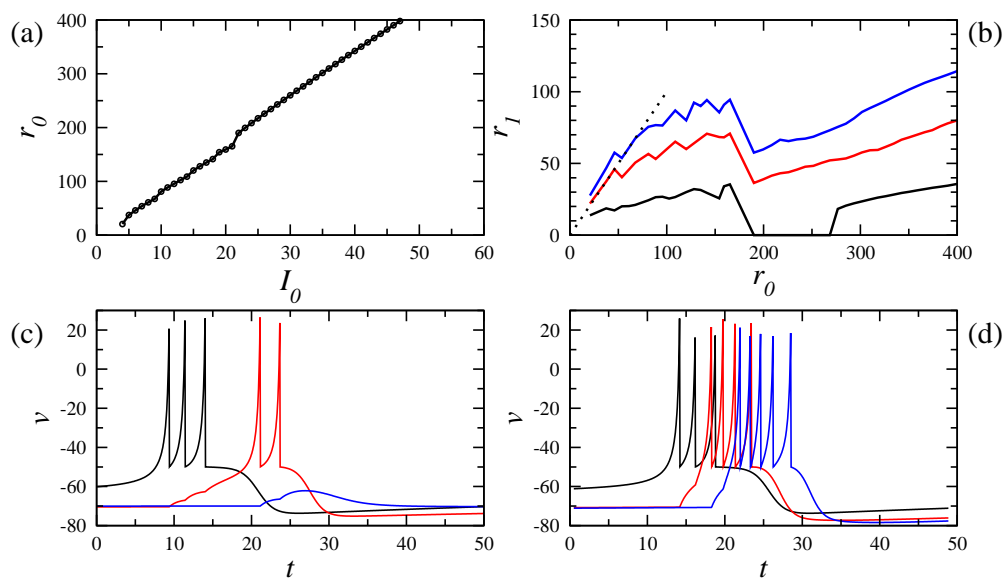s_{10}
s_{12}
1
s_{21}
2
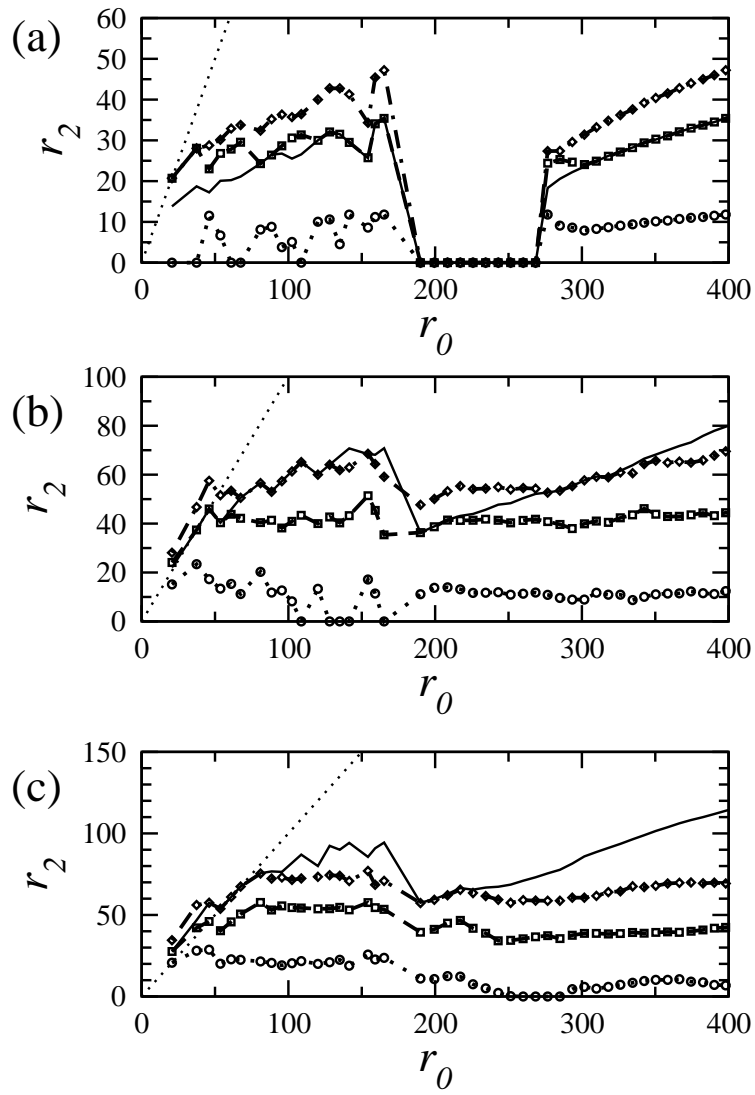neuron 1
neuron 2
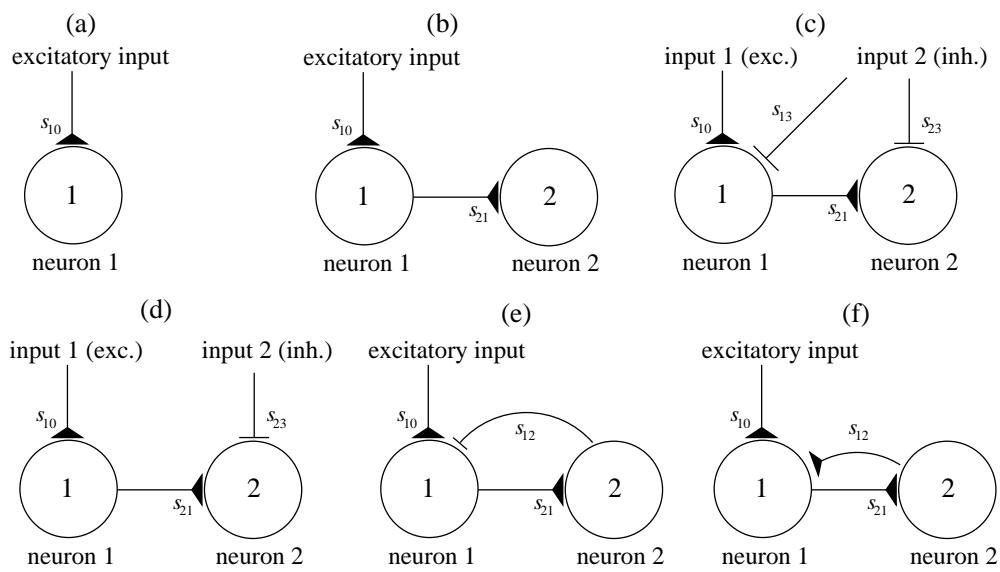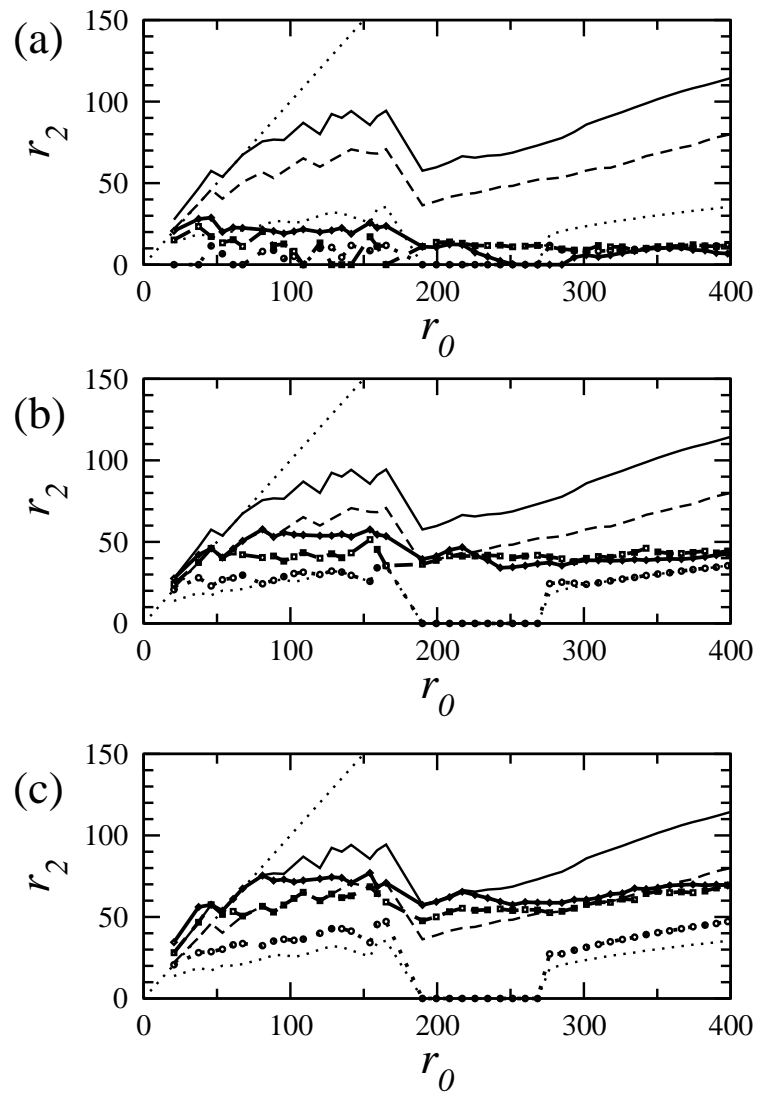
Figure 1:

Figure 2:

Figure 3:

Figure 4:

Figure 5:

Figure 6:

23

Figure 7:

Figure 8:

Figure 9: